SUBMITTED TO APJ
Preprint typeset using LaTeX style emulateapj v. 10/09/06

THE CEPHEID PHASE LAG REVISITED

RÓBERT SZABÓ[1], J. ROBERT BUCHLER AND JUSTIN BARTEE
Department of Physics, University of Florida, Gainesville, FL 32611-8440
Submitted to ApJ

ABSTRACT

We compute the phase lags between the radial velocity curves and the light curves $\Delta\Phi_1 = \phi_1^{V_r} - \phi_1^{mag}$ for classical Cepheid model sequences both in the linear and the nonlinear regimes. The nonlinear phase lags generally fall below the linear ones except for high period models where they lie above, and of course for low pulsation amplitudes where the two merge. The calculated phase lags show good agreement with the available observational data of normal amplitude Galactic Cepheids. The metallicity has but a moderate effect on the phase lag, while the mass-luminosity relation and the parameters of the turbulent convective model (time-dependent mixing length) mainly influence the modal selection and the period, which is then reflected in the period – $\Delta\Phi_1$ diagram. We discuss the potential application of this observable as a discriminant for pulsation modes and as a test for ultra-low amplitudes (ULA) pulsation.

Subject headings: Cepheids — instabilities — stars: oscillations

1. INTRODUCTION

The relative phase between the luminosity and the velocity curves in classical pulsating variables was a puzzle in the early days of variable star modeling. Because, overall, the pulsations are only weakly nonadiabatic it was expected that the maximum brightness should occur at maximum compression, *i.e.*, minimum radius, whereas in reality it is observed to occur close to maximum velocity. (To avoid confusion we note that in this paper we use astro-centric velocities.) The luminosity thus has a $\sim 90^\circ$ phase lag compared to the one expected adiabatically.

As it became possible to make accurate linear and nonlinear calculations of the whole envelope, including in particular the outer neutral hydrogen region, agreement between modeling and observation was achieved. However, it was Castor (1968) who first provided a qualitative *physical* understanding of this phenomenon. He pointed out that during the expansion phase, for example, the hydrogen partial ionization front moves inward with respect to the fluid, and energy is absorbed in the recombination. Because of this temporary storage of energy (as in the charging of a capacitor) the H acts acts like a low-pass filter, causing a phase lag of close to 90 degrees. However, the exact value of the phase lag depends sensitively on details of the stellar model, and can only be obtained by detailed simulations. An understanding of the phase lag involves physics both in the linear and the nonlinear regimes. This characteristic makes it an ideal benchmark to test existing hydrocodes against observational constraints.

Cepheids are known to have humps or bumps on the light curves, especially near maximum light. Rather than define the phases with respect to maximum light, or some other chosen reference point, it is therefore desirable to define them in terms of a Fourier sum:

$$f(t) = \sum_{k=1}^{n} A_k \sin(k\omega t + \phi_k) \qquad (1)$$

The phase lag $\Delta\Phi_1 = (\phi_1^{V_r} - \phi_1^{mag})$ is thus defined as the difference between the phases of the fundamental components of the Fourier fits of the radial velocity (V_r) and magnitude curves. The two time sequences are of course reduced to the same time origin (epoch).

Good Galactic Cepheid light curve data have been available for a long time, while radial velocity data are more recent. Ogloza *et al.* (2000) have published the phase lags for a set of fundamental (F) and first overtone (O1) Cepheids and have found that for the F Cepheids $\Delta\Phi_1$ is largely independent of pulsational period, with an average value of –0.28, but that for the O1 Cepheids it decreases with period from –0.24 to –0.71.

In this paper we describe the results of an extended survey of the linear and the nonlinear (full amplitude) Cepheid pulsation models, and we revisit the phase lag problem. In our computations we make use of the state-of-the-art Florida-Budapest hydrocode (Yecko *et al.* 1998; Kolláth *et al.* 1998, 2002) which includes a model for turbulent convection.

Our goal is to compare the modeling results with a turbulent convective hydrocode for the phase lag with the available observational data. The last similar systematic phase lag investigation was carried out by Simon & Davis (1983) using early radiative hydrocodes and opacities. Furthermore, the limited number of their models, and the quality of the observations that were available at the time justify a new look at the problem.

2. LINEAR AND NONLINEAR CEPHEID MODELING

With the usual convenient, but excellent assumptions of a chemically homogeneous envelope and a rigid, nonpulsating core, we can then specify a Cepheid envelope by three parameters for a given composition: effective temperature ($T_{\rm eff}$), luminosity (L) and stellar mass (M). The composition is usually specified by the H content X, the metallicity Z and the He content Y=1–X–Z.

Cepheids evolve on tracks that are provided by stellar evolution calculations, and the vast majority of Cepheids are expected to be found on the second, blueward penetration of the IS. Since the Cepheid tracks are more or less horizontal (fixed L) it is customary and convenient to identify these tracks by an M-L relation, $L = L(M; X, Z)$. This reduces the number of stellar parameters by one, and we can thus make one-parameter sequences of models for a given mass M and composition with

Electronic address: rszabo@konkoly.hu, buchler@phys.ufl.edu, bartee@phys.ufl.edu
[1] On leave from Konkoly Observatory, Budapest, Hungary

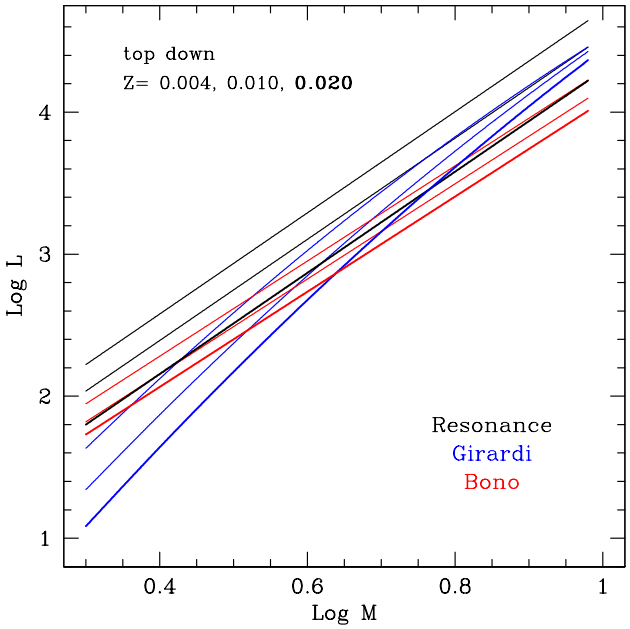

FIG. 1.— The Resonance, Girardi and Bono mass-luminosity relations for Galactic, LMC and SMC metallicity.

$T_{\rm eff}$ as the parameter. The selected *M-L* relation however affects the whole picture from modal selection, to mass-period relation, to phase lags.

In this paper we make use of three different *M-L* relations. These relations are usually obtained from evolutionary calculations. The problems with evolutionary tracks producing Cepheids and the difficulty of deriving mass-luminosity relations are addressed in Buchler & Szabó (2007). Our first *M-L* relation is a fit to the evolutionary tracks with a nonzero overshooting parameter of Girardi *et al.* (2000). Bono *et al.* (2000) give an *M-L* relation that is a fit to their evolutionary tracks without overshooting. One can also bypass evolution calculations and combine observational data with pulsational theory. This has been done for the SMC and the LMC by Beaulieu *et al.* (2001) who derived stellar masses from the observed magnitudes, colors and periods, but reddening errors prevented the extraction of a very tight *M-L* relation. An alternative is to pinpoint the $P_2 : P_0 = 1 : 2$ resonance center from the behavior of the Fourier phase ϕ_{21} as a function of period, and then use linear modeling to match the resonance condition and thus tie down a 'Resonance' *M-L* relation, which is assumed to be linear: $\mathrm{Log}\, L = a + 3.56\, \mathrm{Log}\, M$, where a is 0.7328, 0.96864, 1.1552 for Z = 0.020, 0.010 and 0.004, respectively. We refer to it as the *Resonance M-L* relation. (In this paper we label the modal periods with numeral subscripts, *i.e.*, 0 for F, 1 for O1, etc.)

The three *M-L* relations are displayed in Fig. 1. For Z=0.020 the Resonance *M-L* relation runs close to the Bono relation in the low mass regime, while the Girardi relation predicts much lower luminosity. In the high mass range ($M > 5.8 M_\odot$) the Resonance *M-L* relation runs between the Girardi and Bono formulae for this metallicity. This characteristic has led us to choose the Resonance *M-L* relation as the reference throughout this paper. The sensitivity to the form of the *M-L* relation will be discussed in Sec. 4.3.

The mass range of our survey extends from a lower M of $2.0 M_\odot$ to an upper M that we vary with the metallicity and observational constraints, *i.e.*, the observed longest period pulsation, and is $9.5 M_\odot$, $7.5 M_\odot$ and $6.5 M_\odot$ for Galactic, LMC and SMC variables, respectively. The mass increment is $0.5\ M_\odot$ between the sequences. The luminosity is obtained from the *M-L* relation. The temperature range covers the whole classical instability strip (**IS**), and subsequent models are computed 100 K apart.

TABLE 1
TURBULENT CONVECTION PARAMETERS

Set	α_d	α_c	α_s	α_ν	α_t	α_r	α_p	α_λ
A	2.177	0.4	0.4330	0.12	0.001	0.4	0.0	1.5
B	2.177	0.4082	0.4082	0.25	0.0	0.0	0.0	1.5

In our calculations we employ the Florida-Budapest hydrocode (Yecko *et al.* 1998; Kolláth *et al.* 1998, 2002) to produce equilibrium Cepheid models, to perform their linear stability analysis and to compute full amplitude pulsations. This code incorporates a time-dependent mixing length model for turbulent convection (Yecko *et al.* 1998). The G91 OPAL (Iglesias & Rogers 1996) with solar element abundances (Grevesse & Anders 1991) and Alexander & Ferguson (1994) opacities are used. The equation of state and the opacity are given in terms of the usual composition variables, X, Y and Z.

The values of the turbulent convective (α) parameters in the code affect most of the observables of Cepheid models, such as the width of the IS, the shape of the light and radial velocity curves, the amplitudes, the locations of the resonances, the maximum overtone period, just to name a few. It has been found that very different parameter sets can give surprisingly similar results. But a global calibration of the turbulent convective parameter set has not been performed yet, because of the huge computational task. Therefore we restrict ourselves to only two sets, which are presented in Table 1. The 8 parameters are dimensionless, of order of unity, but they obey a scaling invariance (Kolláth *et al.* 2002).

The linear code provides the radial displacement, velocity, temperature and turbulent energy eigenvectors for all the radial pulsation modes at any point, and in particular in the photosphere. From these we can compute the luminosity and magnitude eigenvectors, and then the phase lags $\Delta\Phi_1$. In this paper we are interested in periodic F, O1 and O2 pulsations (limit cycles).

The equilibrium models are initiated with a velocity kick in one of the eigenmodes and the desired full amplitude (limit cycle) pulsations are computed with our hydrocode. The regime where the F and O1 modes are simultaneously linearly unstable is well known to split into two types, depending on the stellar parameters, namely a double-mode regime, where both modes achieve full amplitude, and a hysteretic regime – the 'either–or' regime in the pulsation jargon – where F and O1 limit cycles coexist, and the initial kick determines which of the two limit cycles is attained. A similar split occurs for the O1 and O2 modes. (In some narrow regions the situation can be even more complicated, *e.g.*, Kolláth *et al.* (2002)). The double-mode pulsations (also called beat pulsations) are not of interest to us here, but are taken up in a subsequent paper. The desired phase lags $\Delta\Phi_1$ are obtained from the magnitude and V_r curves of the computed limit cycles through an 8th order Fourier fit (Eq. 1).

3. MODAL SELECTION – THE BIFURCATIONS

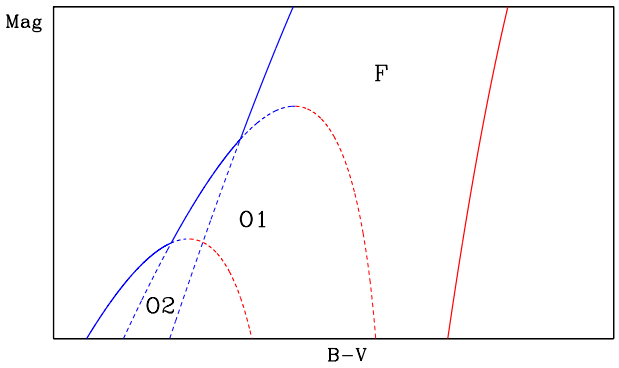

FIG. 2.— Schematic HR diagram showing the *linear* instability strips of the fundamental (F), first (O1) and second overtone (O2) modes. At the solid lines the linear and nonlinear edges coincide.

First we recall the general topography of the *linear* IS shown schematically in an HR on Fig. 2. In the domain of astrophysical parameters that are relevant for Cepheids, only the F, O1 and O2 modes are unstable. As to the definitions of linear and nonlinear edges we refer to the literature, *e.g.*, (Stellingwerf 1975; Buchler & Kovács 1986), Szabó & Buchler (2007, in preparation) and in particular Figs. 4 and 5 in Feuchtinger *et al.* (2000) whose notation we will use here, namely **L** for linear and **N** for nonlinear, in connection with **BE** for the blue edge and **RE** for the red edge. Fig. 2 shows that the region of linear instability of the F mode extends to very high luminosities. That of the O1 mode resembles a sugar cone, thus with a maximum luminosity, which overlaps with the F IS. Similarly the O2 IS sugar cone, with a yet lower maximum luminosity, overlaps with both the O1 and F ISs. Along the solid lines the linear and nonlinear edges coincide, and the pulsation amplitudes vanish there (See Buchler & Kolláth (2002) for a more thorough discussion of how the behavior at the edges of the IS is affected by stellar evolution). The dotted parts of the linear instability boundaries are not real edges because an evolving star that is pulsating in a given mode undergoes a switch (bifurcation) to another type of pulsation before it can reach the dotted line corresponding to the original pulsation mode. The substructure in the topography of the IS will be discussed in a paper on Beat Cepheids (Szabó & Buchler 2007, in preparation).

For the purposes of this paper we note that because the star pulsates with infinitesimal amplitude near the solid edges, the linear and nonlinear phase lags therefore approach each other. All other mode switching occurs with finite amplitude and the linear and nonlinear $\Delta\Phi_1$ differ therefore at the bifurcation. This behavior will clearly be visible in the subsequent figures. Thus for example, a star on a blueward horizontal track at high luminosity in Fig. 2 starts to pulsate with infinitesimal amplitude when it crosses the FRE (the solid line on the right) and stays in this mode until it reaches the FBE (solid line) on the left where its pulsation amplitude goes to zero. The linear and nonlinear $\Delta\Phi_1$ should thus be equal to each other both at the FRE and at the FBE. In contrast, a star on a blueward track at mid-magnitude in Fig. 2 similarly starts to pulsate when it crosses the FRE (the solid line on the right), but it bifurcates to some other pulsational state before it reaches the LFBE (the dotted line corresponding to the F mode). The amplitude of the pulsation does not go to zero at the switching which has as a consequence that the linear and nonlinear $\Delta\Phi_1$ are different. Finally, we note that because of the *M-L* relation, the ordinate in the schematic Fig. 2 could also represent the stellar mass *M*.

In the two hysteretic regimes, where the pulsation is periodic, it can be in either the F or the O1 mode, or it can be in either the O1 or O2 mode, respectively. In this regime we include the corresponding model in both the F and the O1 set of pulsators. The double-mode pulsations of two types that have been encountered, namely F&O1 and O1&O2, are ignored here because of their multi-periodic nature. They will be discussed in a separate paper (Szabó & Buchler 2007, in preparation). The temperature range of the double-mode region is typically less then 100*K*, therefore the exclusion of these models has little effect on the results of this paper.

4. LINEAR AND NONLINEAR PHASE LAGS

4.1. *Results*

The general picture of the theoretical linear and nonlinear phase lags is displayed in Fig. 3a. These results are obtained by using the Resonance *M-L* relation, the turbulent convective parameter set A (Table 1), and a Galactic metallicity (Z=0.020). Below we investigate how each of these three choices affects the results. The phase lags are plotted as a function of the logarithm of the period of the excited mode (The models in the 'either F or O1' regime appear twice, once under P_0 and once under P_1). Our models form one-parameter sequences at a given *M*, and thus $L = L(M)$, with $T_{\rm eff}$ as the variable parameter. The masses of the sequences run from $2.5M_\odot$ to $9.5M_\odot$, with a $0.5M_\odot$ increment, and are labeled by the small (integer) numbers. The F, O1 and O2 groups start with the same masses on the left. The dotted lines depict the linear phase lags of the linearly unstable models, while the thick lines correspond to the nonlinear phase lags, *i.e.*, those of the limit cycles. (Some inter/extrapolation has been done near the edges.)

In Fig. 3a one can identify the three separate clusters that correspond to the F, O1 and O2 radial pulsation modes of the sequences of models. For high masses, the nonlinear sequences follow the linear ones of the same mass. At a certain mass O1 pulsation appears, thus the nonlinear F curves stop before reaching the FBE, and the sequence continues in the corresponding O1 curve. In the 'either-or' regions, the same model contributes to two pulsational modes. The same thing happens where the sequences change from O1 to O2 pulsation at even lower mass. Therefore the F and O1 sequences seem to be increasingly incomplete toward the short periods at low mass. At the lowest mass regime, the models reach the blue edge pulsating in the O2 mode.

As expected, the F mode pulsations cover the broadest range in period and in mass, as well as in phase lag. We remark in advance that when comparing the theoretical values of the phase lags to observations the most relevant part of these arches are the broad vicinity of their maxima, because the long 'legs' on the high period (right) side of the sequences are associated with low pulsational amplitudes, near the FRE. We will discuss this issue later on. Along the sequences the dots mark 100 K intervals which allows one to see that the models are not equidistant along the $\Delta\Phi_1$ in Fig. 3, but that they crowd toward the center of the IS and are increasingly spaced out toward the FRE. The FRE is the lower envelope of the F sequences on the figure, corresponding to infinitesimal pulsational amplitude. The spacing is increasing toward the low mass models, too. The maximum F phase lags of the models thus lie close to zero, while the bulk of our models are in the –0.1 to –0.4 range.

The phase lags for the O1 and the O2 pulsations of the sequences are located lower on the diagram to the left. With

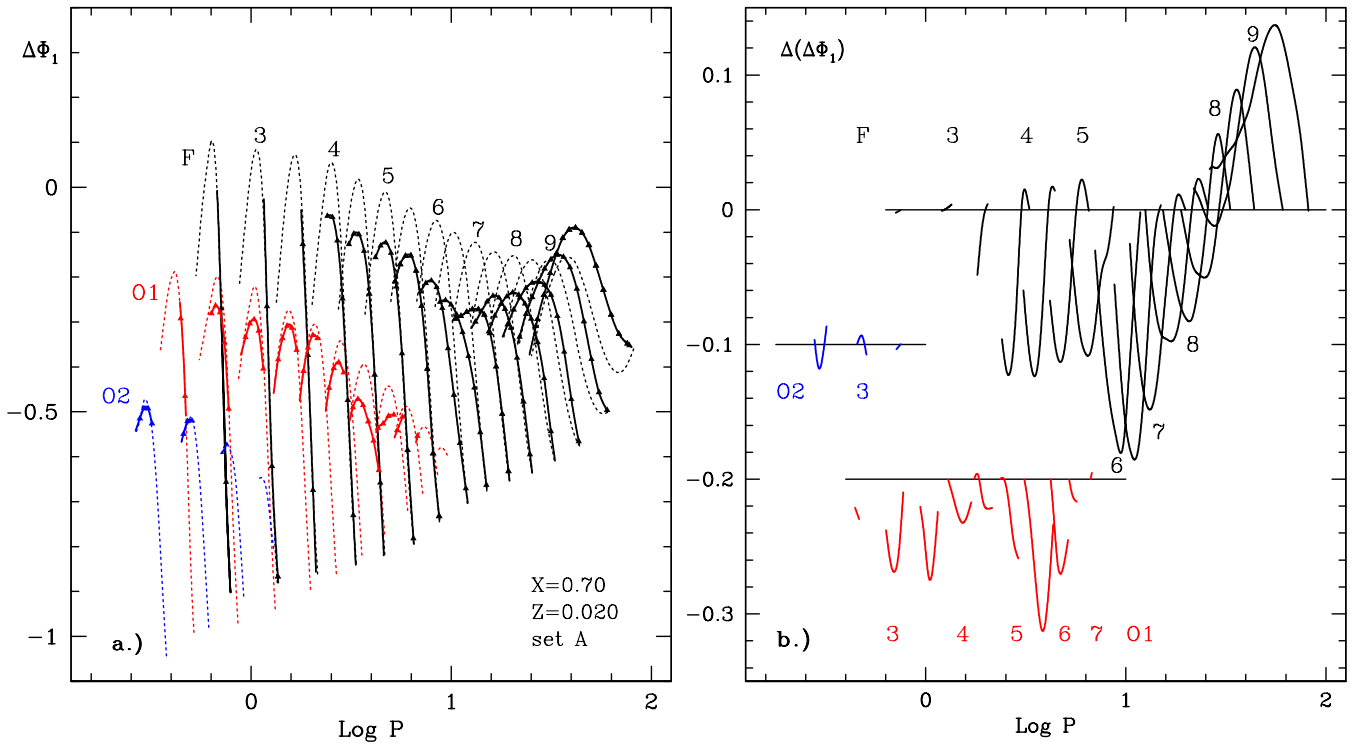

FIG. 3.— **a.)** Linear and nonlinear phase lags of sequences of equal mass Galactic Cepheid models. The mass labels appear on top. The dashed lines denote the linear phase lags of linearly unstable models, the thick lines denote the nonlinear (limit cycle) phase lags. The triangles along the model sequences denote 100K intervals in $T_{\rm eff}$. The Resonance *M*-*L* relation was used along with the α parameter set A (Table 1). **b.)** The difference between the nonlinear and linear phase lags ($\Delta(\Delta\Phi_1)$) for the same models, as a function of the pulsational period. The O1 and O2 models are shifted vertically by –0.2 and –0.1, respectively for clarity. See color version of the figures in the online edition.

the chosen set A of α parameters the maximum O1 period is $\sim 7^d$, and the maximum O2 period is $\sim 1^d$. The Cepheids pulsating with the maximum O1 period are close to the LOBE, and therefore low amplitudes are expected to hamper their discovery (see Feuchtinger *et al.* (2000) for a similar comment). The same argument applies for the maximum O2 period, although no Galactic O2 Cepheids have been found to date.

We need to point out that this maximum O1 period is sensitive to the turbulent convective parameters that we use. This will be discussed in Sec. 4.4 and a thorough calibration will be attempted in Szabó & Buchler (2007, in preparation). We note however, that our phase lag results do not seem very affected by changes in αs as long as we use a parameter combination that reproduces the maximum O1 period.

4.2. *Resonances*

It is well known that internal resonances cause structure in the Fourier coefficients *vs.* period or some other parameter, (*e.g.*, Buchler (1993)). Thus the light curves of RR Lyrae who have no low-order internal resonances exhibit very smooth Fourier decomposition coefficients (ϕ_{21}, R_{21}, etc), whereas the Cepheids which span a much wider range of M, L and $T_{\rm eff}$ encounter a number of such resonances during their evolution though the IS (see for example Fig. 4 in Buchler (1997)). We will see that these resonance characteristics are important in this study.

As we mentioned earlier, the differences between the nonlinear and linear phase lags, $\Delta(\Delta\Phi_1)$, vanish at the IS edges. This is depicted on Fig. 3a, especially for the F and O1 sequences. The $|\Delta(\Delta\Phi_1)|$ are very small for the O2 pulsators which have very low amplitudes. Generally, one expects that the larger the amplitude the larger the difference between the linear and nonlinear quantities such as the phase lag. This simple argument may break down where there are resonances which distort the light and radial velocity curves.

The largest $|\Delta(\Delta\Phi_1)|$ are found around $P_0 = 10^d$ for the F pulsators, but it is not immediately clear whether this is related to the well-known $P_2 : P_0 = 1 : 2$ resonance, or whether it is just a broad minimum occurring there by coincidence, as part of a general trend running through the whole mass range. To resolve the issue, we display the $\Delta(\Delta\Phi_1)$ values on Fig. 3b. The O1 and O2 sequences are shifted vertically for clarity. The $\Delta(\Delta\Phi_1)$ are positive for the highest mass values, and tend to be negative for lower masses. For a given mass sequence its absolute value is largest toward the middle of the instability strip. We point out that this figure is very similar for the $\Delta(\Delta\Phi_1)$ for LMC and SMC metallicities that are discussed in Sec. 4.5.

The $\Delta(\Delta\Phi_1)$ tend to be more negative in the vicinity of the resonance, and they do not extend to the positive region. On the low period side $\Delta(\Delta\Phi_1)$ changes abruptly due to the distortion of the light and velocity curves that is caused by the resonance. Based on these findings, we conclude, that the $P_2 : P_0 = 1 : 2$ resonance has a noticeable effect on the phase lags. Namely, an additional dip appears on the upper envelope of the arched nonlinear phase lags which is very pronounced around the resonance center. The Log P – $\Delta(\Delta\Phi_1)$ diagram shows, that the resonance related distortion plays an equally important role in shaping the phase lag curves as the amplitudes themselves. The same resonance behavior will be noticed in the LMC and the SMC metallicity models around the apposite resonance periods confirming our argument.

Similarly, we believe that the surprisingly large $|\Delta\Phi_1|$ that are found for the O1 modes of the 5.5 $M_\odot$ sequence of are associated with the $P_4 : P_1 = 1 : 2$ resonance near an overtone period $P_1 = 4^{\rm d}.2$ period. This resonance causes the 'either or

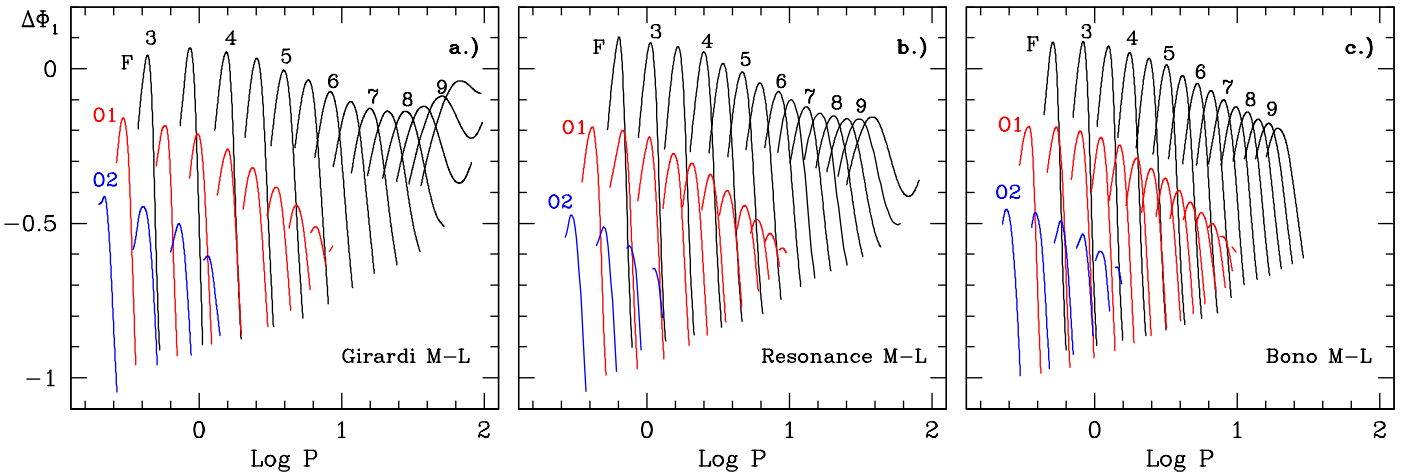

FIG. 4.— Linear phase lags for Galactic metallicity (Z=0.020) with three *M-L* relations: **a.)** Girardi, **b.)** the Resonance *M-L* relation, and **c.)** Bono, for the α parameter set A.

region' to broaden to a width of several hundred K (Szabó & Buchler 2007, in preparation), which is in turn reflected in the much longer O1 phase lag curve. The much shorter $6M_{\odot}$ curve is still affected by the resonance, as its strange shape and the large $\Delta(\Delta\Phi_1)$ indicate.

The effect of these resonances can also be witnessed on the amplitude behavior which is discussed further in Sec. 5.

4.3. *Effects of the M-L relation*

Fig. 4 compares the linear $\Delta\Phi_1$ for the three *M-L* relations that we have described in §2. In order to avoid overcrowding we plot only the linear phases lags. The overall difference between the nonlinear and linear lags are found to be similar to what we have seen in Fig. 3a for the Resonance *M-L* .

One immediately notices that the effect of the three *M-L* relations is most prominent in the high mass regime, where the highest periods are quite different. The Bono *M-L* relation has lower luminosity than the other two, and it would require a much higher mass ($> 10M_{\odot}$) to reach the 100^d fundamental period limit to which the $9.5M_{\odot}$ sequence rises for the Resonance *M-L* . On the low-mass and low luminosity end the $1\overset{d}{.}0$ F period occurs for 3.50, 3.00 and $3.25M_{\odot}$ Cepheids, for the Girardi, Resonance and Bono *M-L* relations, respectively, as one would expect from Fig. 1.

With the Girardi relation the $\Delta\Phi_1$ values of the models turn upward (especially on the low-temperature (right) side). The same trend is visible with the Resonance *M-L* relation but does not occur with the Bono one, again consistently with the behavior of the *M-L* relations.

We conclude that the effect of the *M-L* relations on the $\Delta\Phi_1 - \log P$ diagram occurs indirectly through a modification of the mass-period relation.

Generally the observed phase lags, which are shown in Fig. 4, and the mass-period distribution show good agreement with the models obtained by the Girardi and the intermediate *M-L* relations, but disagree with the Bono relation at high mass.

4.4. *Effects of the α Parameters*

The two sets of convective α parameters that we use here are given in the Table. The main difference lies in the amount of turbulent viscosity (α_ν) which is higher for set B. Set A features a small amount of overshooting (α_t) and Péclet-correction (α_r), which accounts for the decrease of convective efficiency when radiative losses are important. Despite the smaller turbulent viscosity in set A, the models computed with these parameters show lower luminosity and velocity amplitude by a factor of two compared to models in set B. The smaller α_ν is overcompensated by the remaining parameters.

Fig. 5 compares the linear and nonlinear phase lags computed with set A (a.) panel) and set B (b.) panel) convective parameter sets. The Resonance *M-L* relation and a Galactic metallicity ($Z = 0.020$) have been used in both.

The shape of the phase lag curves is similar on the two panels, but the range of the phase lags is smaller for set B. The difference has to do with the lower pulsation amplitudes that are found for set B. Another noticeable feature is the smaller difference between the linear and nonlinear phase lags for panel B. The underlying cause is again the too low amplitude with the set B parameters, because this difference depends on the nonlinear effects, *i.e.*, the magnitude of the amplitude.

The convective parameters affect the modal selection. Our main concern has been to reproduce the observed maximum O1 period ($7\overset{d}{.}57$ for V440 Per). We find that the longest period among the nonlinear overtone models is $7\overset{d}{.}7$ for the set A models, and a very small value for the set B parameter choice (less than 3 days) that is unacceptable on observational grounds. The difference in modal selection manifests itself in the O2 pulsation, too. For set A, there is (pure) second overtone pulsation for mass lower than $3.5\,M_{\odot}$. However the radial second overtone mode is linearly unstable only for masses below $2.5\,M_{\odot}$ in set B, and no O2 pulsation was found in the models in the hydro grid in this case. This means, that if O2 pulsation exists there, it would occupy a rather narrow temperature range.

Our experience is that, as long as they are capable of reproducing the observed mode selection patterns, the turbulent α parameters do not have a major effect on the phase lags.

4.5. *Effects of the Metallicity*

We have adopted here the following composition pairs (X, Z) = (0.700, 0.020), (0.716, 0.010), (0.726, 0.004) as 'canonical' values when computing Galactic, LMC, and SMC models, respectively.

In Fig. 6 we display the linear and nonlinear phase lags for the LMC (a.) panel) and SMC (b.) panel) metallicities. For short periods the phase lag is insensitive to the metallicity, but for high periods (*i.e.*, high masses) *lowering the metallicity causes the theoretical F phase lags to shift up-*

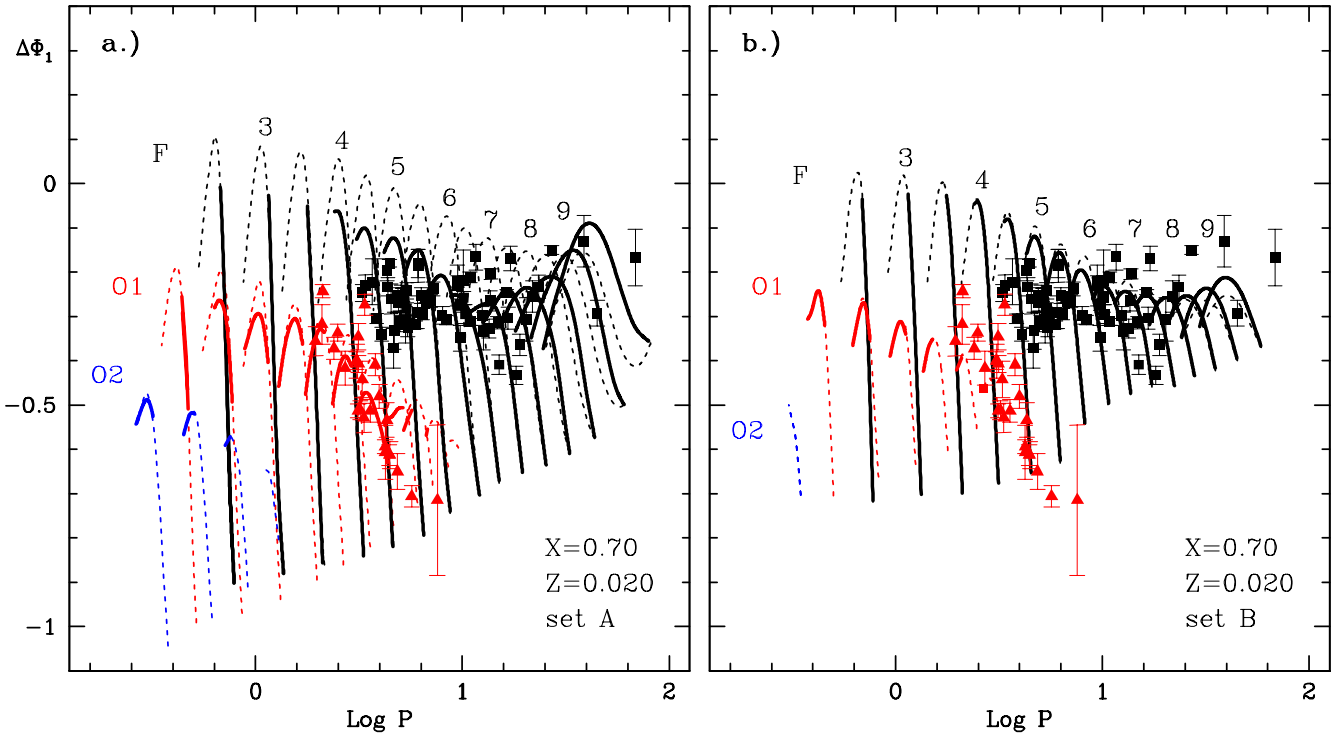

FIG. 5.— Linear and nonlinear *Galactic* phase lags computed with two different α parameter combinations a.) set A and b.) set B. and using the Resonance *M-L* relation. Dashed lines: linearly unstable models, thick lines: nonlinear (limit cycle) phase lags. The observed phase lags with error bars are overplotted for F (squares) and O1 (triangles) Cepheids (Ogloza *et al.* 2000; Moskalik & Ogloza 2000). See color version in the online edition.

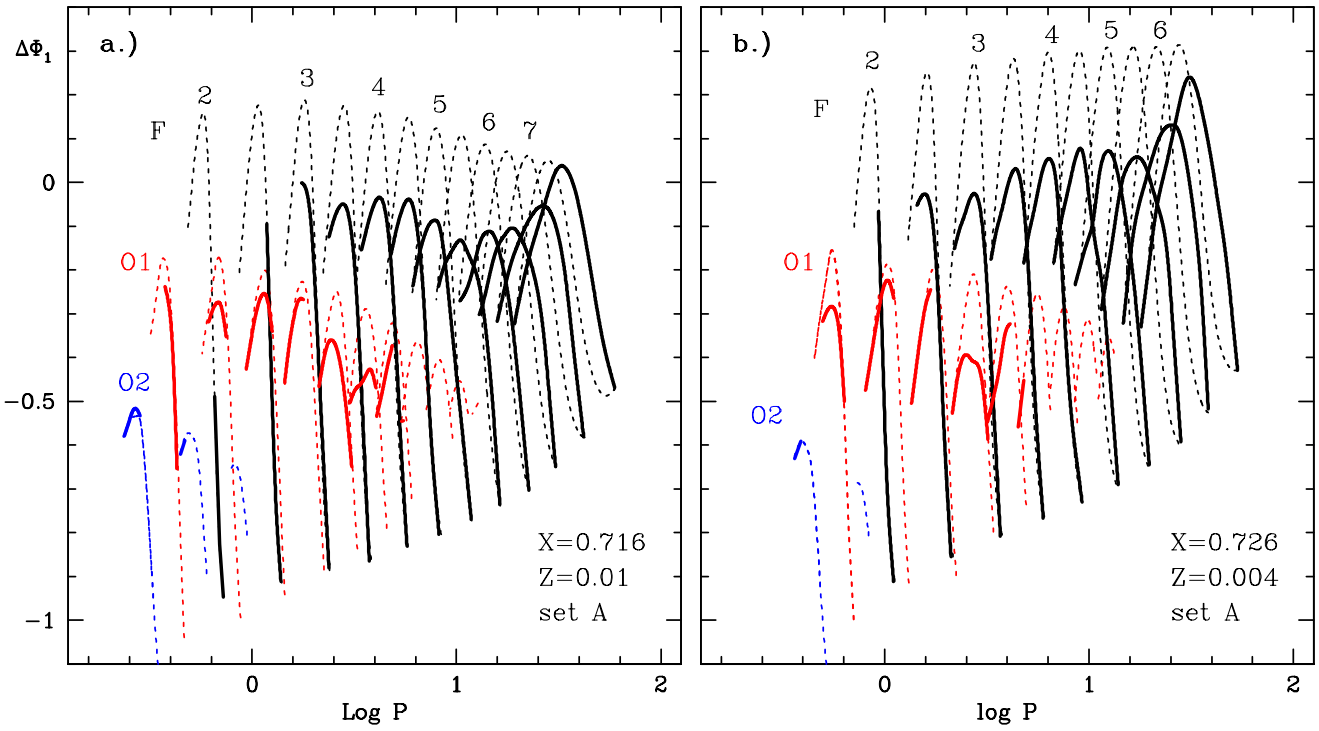

FIG. 6.— The effect of metallicity on the phase lags. LMC and SMC models are shown on panel a.) and b.), respectively. Dashed lines: linearly unstable models, thick lines: nonlinear (limit cycle) phase lags. The results are obtained with the Resonance *M-L* relation and the α parameter set A.

ward, and even causes a reversed sign. The same trend can be seen for O1 models, although to a lesser extent. We note that the $P_2 : P_0 = 1 : 2$ and $P_4 : P_1 = 1 : 2$ resonances mentioned in Sec. 4.2 have very similar effects on the phase lag of the lower metallicity model sequences. Unfortunately no observational extragalactic $\Delta\Phi_1$ are available to date on which we could test our predictions.

The maximum period of the possible O2 pulsation decreases with decreasing Z, but observationally, a number of O2 and O1&O2 double mode Cepheids are known in the Magellanic Clouds in contrast to the Galaxy. This does not cause a problem though, because the evolutionary tracks also shift with Z. Also, our maximum predicted O2 periods are close to maximum O2 period reported for O1&O2 double mode Cepheids in the LMC (Soszynski *et al.* 2001) and in the SMC (Udalski *et al.* 1999).

So far we have only considered a solar mix where the 'metals' are lumped collectively into Z. However, it has been found that deviations from the standard solar chemical composition (Grevesse & Anders 1991) play a nonnegligible role in beat Cepheid period ratios (Buchler & Szabó 2007). We have therefore also computed the linear phase lags for a model sequence with the same opacities as used and described in Buchler & Szabó (2007), namely Fe group element number densities arbitrarily reduced to 75% at fixed Z. The phase lags are found to be largely insensitive to the chemical buildup, the difference is largest for high mass models, being less than 0.01, and in general it is much less.

After having demonstrated that the phase lags are moderately sensitive to metallicity and that they implicitly depend on the *M-L* relation and the turbulent convective parameters, we examine other possible physical and numerical effects on the Cepheid phase lags. For these tests we have computed only *linear* models, because the relationship between nonlinear and linear phase lags is not strongly affected, and this will therefore not significantly alter our conclusions.

4.6. *Stellar Rotation*

In this section we consider the effect of *stellar rotation* because it has the effect of rearranging the stellar structure, and can cause slight changes in the phase lags. However, since we do not have the 3D code to conduct a proper calculation of the effects of rotation, we resort to an expedient subterfuge which we expect to be accurate enough as an order of magnitude estimate. As in Buchler & Szabó (2007) and references therein we incorporate in our 1D hydrocode a radial pseudo-centrifugal force of the form ($F = \omega^2 r$) which, if anything, is likely to overestimate the effects of rotation. We find that even up to 20 km s^{-1} rotation, the phase lags are indistinguishable from the nonrotating ones, except perhaps for the highest masses ($> 9M_\odot$), where the relative difference is still only 0.02. We note that observed Cepheid rotation rates ($v_{rot} \sin i$) are usually less than 20 km s^{-1} (Nardetto *et al.* 2006).

4.7. *Numerical Resolution*

Finally, we have tested the effects of the numerical resolution of the models. In this work we have used 120 zones in our models, which is sufficient to generate decent light curves. As the phase lag itself is sensitive to the structure of the outer stellar layers, different zoning in this region can potentially influence the lag between the velocity and luminosity maxima. We have recomputed some of our Galactic models with 80 and 300 zones. The linear phase lags turned out to be rather insensitive to the zoning. The difference is the smallest for the low period models, and increases toward higher masses. The maximum deviation is $\lesssim 0.02$. Therefore we conclude that different model zoning has practically no influence on $\Delta\Phi_1$.

5. PULSATION AMPLITUDES

So far we have compared *bolometric* theoretical light curves to observed *V magnitudes* when constructing the *phase lags*. In principle, this inconsistency could cause a problem. Obviously the velocity curves are free from this caveat. However, we think that V phase lags are close to their bolometric counterpart, because the $T_{\rm eff}$ of the Cepheid variables ensures that the maximum of their spectral energy distribution is close to the V band. The ϕ_1^{mag} values for V and I, for example, are indeed found to be very close (Ngeow *et al.* 2003). For a more detailed comparison of the V, B, R, I and bolometric light curve parameters we refer to Simon & Moffett (1985).

However, in order to compare our computed amplitudes to the *observed Galactic amplitudes* we need to convert from our bolometric amplitudes to V amplitudes: $M_V = M_{bol} + BC$. For this transformation we follow Kovács (2000), *viz.*

$$BC = 2.0727\Delta T - 8.0634(\Delta T)^2 \quad (2)$$

$$\Delta T = \mathrm{Log}\, T_{\rm eff} - 3.7720 \quad (3)$$

These fits to the static atmosphere models were derived for Beat Cepheids, but (Beaulieu *et al.* 2001) obtained similar formulae for a broader mass range, the difference being only a small systematic shift between the two ($\Delta \mathrm{Log} L = 0.02$).

On Fig. 7 the A_1 Fourier coefficients of the V light curves are shown for the Ogloza *et al.* (2000) sample together with our full amplitude models. The lowest amplitude O1 Cepheid on the figure is α UMi (Moskalik & Ogloza 2000), included here to complement the observed sample. F Cepheids are denoted by squares, overtones by triangles. The A_1 amplitudes are plotted for our model sequences with $4M_\odot$ to $9.5M_\odot$ for F, and with 4 to $7M_\odot$ for O1 models, computed by using the Resonance *M-L* relation and set A of convective parameters. Since we have not computed nonlinear model pulsations at very low amplitude, we have extrapolated our results to zero amplitude, where applicable, *i.e.*, at the F red edge and at the O1 blue edge.

Fig. 7 shows good agreement between the model calculations and the observations. The only small discrepancy is that the O1 Cepheids do not seem to extend to quite high enough periods, but this partially is due to the coarse grid we used (100K). Because of this, for the $7.5M_\odot$ sequence we do not find stable nonlinear O1 pulsation, while by using a finer grid we could find a narrow temperature range of overtone pulsation.

It's important to notice that Fig. 7 also appears to show a large observational bias toward large amplitude Cepheids, especially among the fundamental mode pulsators. This fact has important consequences for the observed phase lag distribution. This issue is discussed in Sec. 6.

We now turn to the effects of resonances on our amplitude diagram. The action of the $P_2 : P_0 = 1 : 2$ resonance between the F mode and the second overtone, which is at the origin of the well known Hertzsprung progression, is quite visible near $P_0 = 10^d$ in the M=$6M_\odot$ sequence. It causes a dip in the A_1 values. Our models duly follow the observed amplitude minimum.

A corresponding 'overtone' resonance between the fourth and first overtone $P_4 : P_1 = 1 : 2$ appears at $P_1 = 3\overset{\mathrm{d}}{.}5 - 4\overset{\mathrm{d}}{.}0$ in

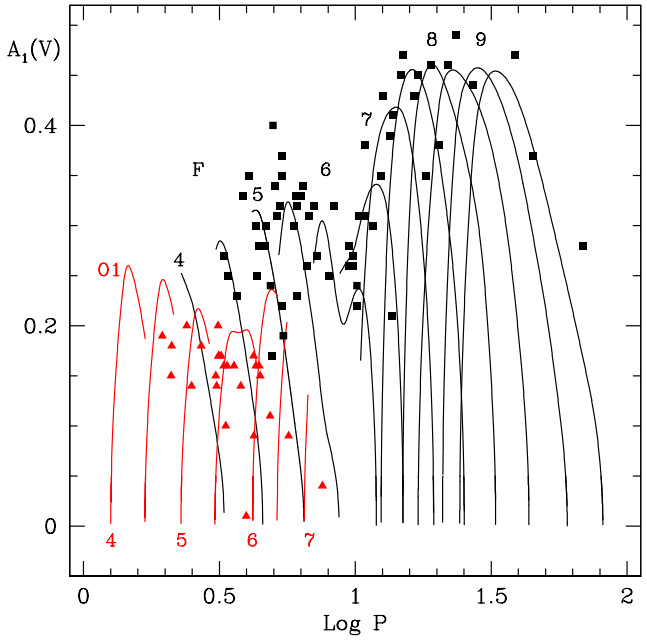

FIG. 7.— Observed and theoretical values of the $A_1(V)$ Fourier amplitude, obtained with the Resonance *M-L* relation and the α parameter set A. The theoretical F models are for our sequences with masses from $4M_\odot$ to $9.5M_\odot$. The overtone sequences which are located at the left lower side, correspond to sequences with masses ranging from $4M_\odot$ to $7M_\odot$. Observed $A_1(V)$ values from the Ogloza *et al.* (2000) sample are overlaid for the F (squares) and O1 (triangles) Cepheids.

the O1 sequences of the M=5.5$M_\odot$ sequence. In this case one has to keep in mind that it is easier to locate the resonance position from the velocity curves than form the light curves. Feuchtinger *et al.* (2000) found the resonance to be centered on $4\overset{d}{.}2$ (although with a slightly different *M-L* relation). The small distortion and the larger dip between the M=5.5 and M=6$M_\odot$ overtone amplitude curves corresponding to this resonance are not seen in the observed sample. The likely reason is the small number of observed O1 Cepheids, and the uncertain mode identification in Galactic Cepheids.

The $P_3 : P_0 = 1 : 3$ resonance (Moskalik & Buchler 1989; Antonello & Morelli 1996) has no visible effect, neither on the computed phase lag nor on the $A_1(V)$ diagrams. Moskalik & Buchler (1990) showed that another possible resonance, $P_1 : P_0 = 2 : 3$ (Antonello & Morelli 1996) has no effect unless it destabilizes the F limit cycle, in which case it causes the appearance of slightly alternating pulsation cycles (period doubling). Such pulsations were reported by Moskalik & Buchler (1991) in radiative Cepheid models, but not in the sequences of turbulent models that we have computed here. No observational evidence has yet shown up to corroborate the existence of alternating cycles in Cepheids of this period range.

To conclude, we have shown that the amplitudes of our models reproduce the observed amplitudes, as well as the resonance characteristics. Furthermore, we have pointed out a deficiency of observed small amplitude Cepheids on our amplitude diagram Fig. 7. These features are important regarding the following section, in which the observed and theoretical phase lags are compared, and an explanation is proposed for the observed phase lag distribution for both F and O1 Cepheids.

6. COMPARISON WITH OBSERVATION

6.1. *The fundamental mode phase lag*

At this time only phase lags from Galactic Cepheids have been reported in the literature (Ogloza *et al.* 2000; Moskalik & Ogloza 2000). In Fig. 5a we have plotted these observational Galactic phase lags. The F Cepheids and O1 Cepheids denoted by squares and triangles, respectively. They are superposed on the linear and nonlinear phase lags that we have computed with our 'standard' reference parameters in this paper, namely the convective parameter set A (a.) panel), the Resonance *M-L* relation and a Galactic metallicity ($Z = 0.020$).

In Figs. 3a and 5 it is seen that our model sequences extend over a much broader range of periods than the observational data. The simple reason is that our sequences are not constrained by the evolutionary tracks (except for the *M-L* relation), and thus they cover a much larger range of stellar parameter values (L, M, $T_{\rm eff}$).

In addition, the observed stars strikingly occupy only the upper section of the region in the $\Delta\Phi_1$ *vs.* Log *P* diagram that is permitted by the modeling. This region corresponds to the inside region of the IS; in other words the observed F sample seems to avoid the vicinity of the F red edge (Fig. 3a). We argue that this arises from an observational amplitude bias. Fig. 7 suggests that the low amplitude Cepheids are missing from the observed sample, most likely because of observational selection effects. We note though that there is also a theoretical reason for the absence of low amplitude Cepheids (Buchler & Kolláth 2002). In all our Log P - $\Delta\Phi_1$ figures, Figs. 3a and 4 the bottoms of the downward legs of the fundamental $\Delta\Phi_1$ curves correspond to the FRE and thus to models with pulsation amplitudes that vanish as the FRE is approached. In addition, towards the red edge the phase lags of the F Cepheid models are extremely sensitive to temperature as witnessed from the spacing of the dots in Fig. 3a.

Fig. 8b juxtaposes the theoretical nonlinear F phase lags and the Ogloza *et al.* (2000) sample. As discussed in §4 the F models sequences terminate at finite amplitude at the nonlinear fundamental blue edge (NFBE), because the model sequence switches either to double mode or to O1 single mode pulsation at that point.

Overall the agreement of the model phase lags with the observational ones is good (differences of 0.1 rad translate to only about 6 °). However, a few systematic discrepancies stand out. For example, the observational F Cepheid phase lags fall slightly above the theoretical ones in the middle range of periods. But, from a comparison of Fig. 5a and Fig. 6 we see that this discrepancy would be mitigated or even removed if we decreased the metal content that we have assumed for the Galactic Cepheid models, in line with a recent revision of the solar metal abundances (Asplund *et al.* 2005).

In Fig. 8b lines of pulsation equi-amplitude (cutoffs) are overplotted from $0\overset{m}{.}0$ at the FRE to $0\overset{m}{.}7$. To avoid confusion we caution that these lines refer *only* to the rising parts of the $\Delta\Phi_1$ curves near the FRE. (There may be multiple equi-amplitude lines because the pulsation amplitudes are not just a function of period and $\Delta\Phi_1$; the same amplitude can occur more than once along the same arch, but generally not on the same line.)

Based on Fig. 8b we can see that the lower limit of the observed amplitude distribution is well represented by the $0\overset{m}{.}7$ and $0\overset{m}{.}3$ cutoff lines for $P \gtrsim 10^d$ and $P \lesssim 10^d$, respectively. This dichotomy and the sharp change in the equi-amplitude lines on the $\Delta\Phi_1$ – log P plane around 10 days has its origin

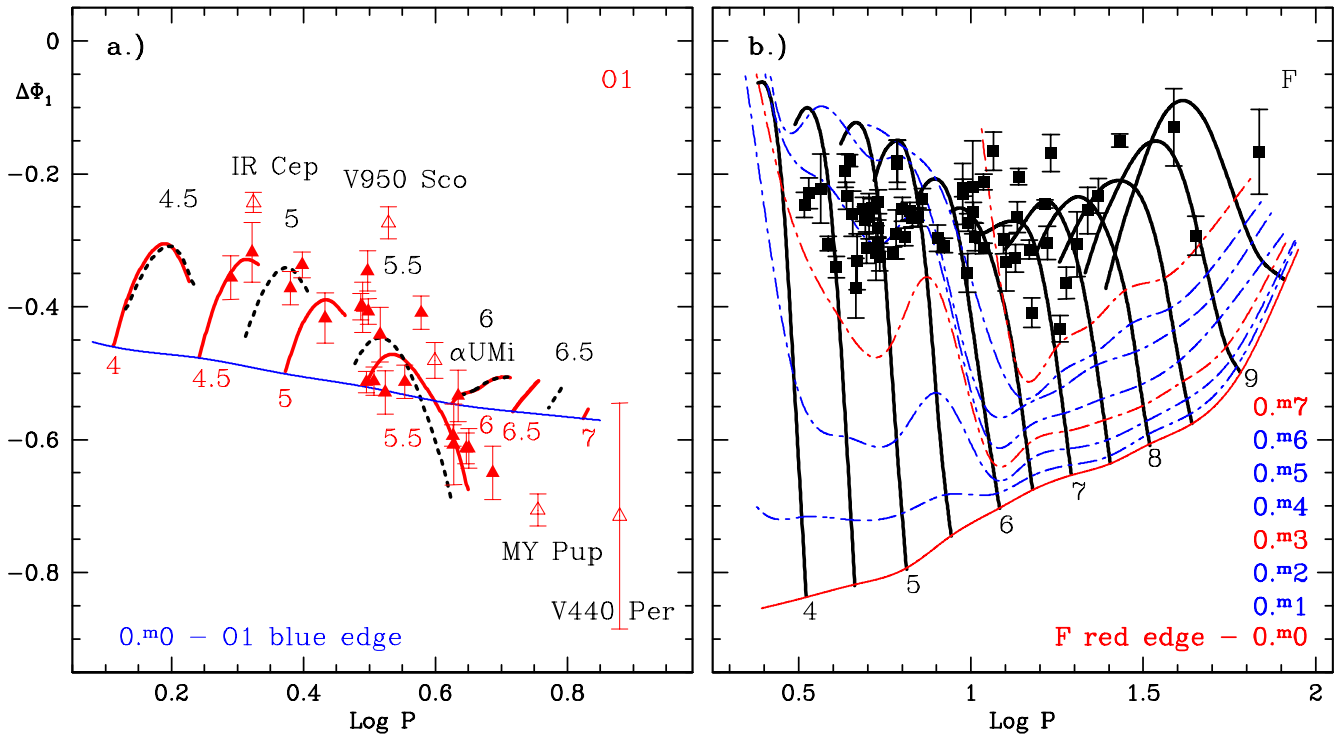

FIG. 8.— Nonlinear (thick lines) phase lags $\Delta\Phi_1$, obtained with he Resonance *M-L* relation, the α parameter set A, and a Galactic composition (bottom mass labels). **a.)**: first overtone Cepheids, **b.)**: fundamental Cepheids. The observational phase lags of the Galactic Cepheids (Ogloza *et al.* 2000) are denoted by triangles and squares, respectively. Individual O1 stars are discussed in the text. On the left panel, dashed lines shows models computed with the Girardi *M-L* relation (top mass labels). On the right, V magnitude cutoff lines (dashed lines) help to define the region of normal amplitude Cepheids (from $0\overset{m}{.}1$ to $0\overset{m}{.}7$). The FRE and the OBE are shown for reference (thin line).

in the $P_2 : P_0 = 1 : 2$ resonance discussed above. Fig. 8b together with Fig. 7 confirm our hypothesis that observational selection effects make the observed sample gravitate toward the high amplitude region.

6.2. *The first overtone phase lag*

On Fig. 8a we display the region of O1 models separately, to avoid overcrowding. Five individual stars that are mentioned below are labeled and plotted with open symbols. As discussed in §4 the O1 models sequences terminate at finite amplitude at the NORE, because the model sequences continue as F single mode pulsation to the right of that point. The $P_4 : P_1 = 1 : 2$ resonance is seen to have a remarkable effect on the M=5.5$M_\odot$ and M=6.0$M_\odot$ phase lags. As is seen most sharply in the 5.5$M_\odot$ sequence the resonance causes $\Delta\Phi_1$ to drop sharply below its value at the blue edge as the nonlinear overtone red edge (NORE) is reached.

In Fig. 8a we have also shown the phase lags of 4.5, 5.0, 5.5, 6.0 and 6.5$M_\odot$ sequences computed with the Girardi *M-L* relations. They are shown as dashed lines. (The 6$M_\odot$ curves are almost indistinguishable for the two different *M-L* relations). Interestingly we find that while the low mass curve is shifted to considerably smaller periods, the envelope of the accessible $\Delta\Phi_1$ curves is affected only slightly. (The reason for the shift to lower periods is of course consistent with Fig. 1 where the Girardi *M-L* relations dip strongly below the Resonance *M-L* relations.

In Fig. 8a the O1 observational points seem to fall a little higher than the ones computed for Galactic models. Again, reducing the metallicity would at least partially mitigate the difference. Most of the discrepancy occurs because of 3 really egregious stars, two with $\Phi_1 > -0.3$ (IR Cep and V950 Sco), and the long period V440 Per with $\Phi_1 < -0.7$. For the first two, strong evidence has been given on the basis of the Fourier decomposition parameters of the light and radial velocity curves that they are O1 pulsators (Moskalik, private communication). However, according to their location in the phase lag diagram, Fig. 5a, at least, they would quite naturally fit in the F, rather than in the O1 group. Alternatively, the disagreement for IR Cep would also disappear if its metallicity was somewhat below the average Galactic metallicity, although this would not apply as well for the longer period V950 Sco.

V440 Per has a low amplitude of A_1=0.095, and an enormous error bar for $\Delta\Phi_1$ (Ogloza *et al.* 2000). It is classified as the longest period Galactic O1 Cepheid. One notes that the O1 Cepheids MY Pup and its immediate neighbors to the left fall right in the middle of the resonance region. The employed *M-L* relation has an effect on the location of this resonance, and this in turn affects the results for $\Delta\Phi_1$. A comparison between the phase lags in Fig. 8a with the Girardi and the Resonance *M-L* relations suggests that an *M-L* relation that lies a little higher than the Resonance *M-L* in Fig. 1 in the 5.5 to 6.0 $M_\odot$ range should push the computed $\Delta\Phi_1$ a little further to the right and improve the agreement for the stars with Log$P_1 > 0.6$, and in particular for MY Pup. However, it is unlikely that this would solve the problem with V440 Per, but we note that the phase lag of this star is compatible with the theoretical ones for small amplitude F Cepheids as seen in Fig. 5a, suggesting that perhaps it is a small amplitude F Cepheid rather than an overtone Cepheid.

α UMi is a well-known Cepheid, most probably pulsating in the first overtone mode. This star has been showing dramatic amplitude changes in the last decades (Turner *et al.* 2005). Currently being a low amplitude pulsator with A_V = $0\overset{m}{.}015$ (Fernie *et al.* 1995), it resides relatively close to our

blue edge on the Log P - $\Delta\Phi_1$ plot (Moskalik & Ogloza 2000). However this agreement should be taken with a grain of salt, because this star can be in the phase of crossing the instability strip for the first time (Turner *et al.* 2005) thus bearing a different *M-L* relation than most of the Cepheids (see e.g. Fig. 2 of Buchler & Szabó (2007)). If this is the case, then evaluating it's position on Fig. 8a would require more computational work with the appropriate *M-L* relation, which is out of scope of this paper.

Finally we note that on a large scale the O1 phase lag distribution appears essentially linear (Ogloza *et al.* 2000). If the three egregious stars are removed from the O1 Cepheids then not only does the observational phase lag distribution appears curved, but that our results closely match its general shape (albeit being a little lower). We have also shown that the curvature of the distribution has its origin in the $P_1 : P_0 = 2{:}3$ resonance.

6.3. *The phase lag of other radially pulsating Cepheids*

Recently ultra-low amplitude (ULA) Cepheids have been discovered in the LMC (Buchler *et al.* 2005). Based on this work we predict that ULA Cepheids pulsating in the F mode and close to the fundamental red edge, would feature a greater (negative) phase lag, and would fall below the current observed range of the regular amplitude Cepheids. Also, ULA O1 Cepheids with periods far from the resonance center would be close to the lower envelope of the predicted phase lag distribution.

Our Fig. 5 offers a method for radial mode identification for Cepheids that is additional and complementary to the usual relative Fourier decomposition coefficients (R_{21}, Φ_{21}, etc). We see that it offers not only a criterion for the F and O1 Cepheids, but also for the elusive Galactic O2 Cepheids. There clearly is an observational bias against low period - low amplitude Cepheids. However, considering the existence of a Galactic O1&O2 beat Cepheid (CO Aur) it is quite likely that pure O2 Cepheids exist as well. The phase lag has the potential of sorting the elusive Galactic O2 Cepheids from O1 Cepheids.

Previous theoretical work on O1 Cepheid pulsations (Antonello & Aikawa 1995) and on O2 Cepheid pulsations (Antonello & Kanbur 1997) Cepheids also discussed the phase lags. However, these authors ignored convection and produced purely *radiative* models, an approximation which makes sense only near the blue edge. The resulting large range of F and O1 phase lags led Antonello & Aikawa (1995) to conclude that $\Delta\Phi_1$ is not a useful discriminator for the pulsational mode. One problem may be that *radiative* models have excessively large amplitudes. Because the nonlinear phase lags depend largely on the amplitude, as we pointed out in Sec. 4.4 we think that to address the phase lag problem correctly, convection can not be left out from the models.

7. CONCLUSION

In this paper we have reexamined the classical Cepheid phase lags, $\Delta\Phi_1 = \phi_1^{V_r} - \phi_1^{mag}$, with our hydrocode which includes a model for turbulent convection.

As expected, the linear and nonlinear (full amplitude) phase lags approach each other when the pulsation amplitude is low, as for example near the fundamental red edge of the instability strip. The nonlinear phase lags generally fall below the linear ones except for high period models where they lie above. The differences between the linear and nonlinear phase lags ($|\Delta(\Delta\Phi_1)|$) are generally at most 0.20 for our Galactic models with the best convective model parameters (set A). In case of lower metallicities, the $|\Delta(\Delta\Phi_1)|$ can be slightly larger.

For Galactic composition *the nonlinear* $\Delta\Phi_1$ *are always found to be negative*, *i.e.*, the radial velocity always lags the luminosity slightly. Lower metallicity models pulsating in the fundamental mode show phase lags that are higher than the Galactic values. We found that high mass models of low metallicity can have positive $\Delta\Phi_1$.

The convective α parameters have a strong influence on the modal selection in the instability strip, as well as on the pulsation amplitude, which is then reflected in the period - $\Delta\Phi_1$ diagram. Similarly, the *M-L* relations have only an indirect effect on the phase lags through a modification of the mass–period relation.

We obtain a good general agreement between the observed Galactic Cepheid phase lag data of Ogloza *et al.* (2000) and our models. For the F Cepheids this agreement could be further improved, when the observed amplitude distribution was taken into account. By applying cutoff magnitude (equiamplitude) lines we could restrict the model phase lags region to the approximate observed range [−0.2; −0.4]. Almost perfect agreement could be achieved by lowering the assumed metallicity of $Z = 0.020$ in accordance with the suggestion of Asplund *et al.* (2005).

Our computed O1 phase lags seem to fall on a steeper relation than the observations, but this discrepancy would be mitigated or removed if we could reclassify two stars, IR Cep and V950 Sco as F Cepheids (even though Fourier decomposition parameters of the light and radial velocity curves indicate otherwise). Furthermore, the phase lag of the outlier, V440 Per, which is normally classified as an overtone, would be compatible with the theoretical phase lag of a low amplitude F Cepheid. With the omission of these three stars our results match the shape of the observational distribution of phase lags.

We have shown that resonances have an impact on the phase lag. The $P_2 : P_0 = 1 : 2$ resonance which is present in the fundamental mode Cepheids at around 10^d period causing the well-known Hertzsprung-progression, has a small effect on the minimum seen in the nonlinear phase lags (Fig. 3a and Fig. 5a). As for the O1 models, the $P_4 : P_1 = 1 : 2$ resonance generates an abruptly wide 'either F or O1' region at around the resonance center. In this region $\Delta\Phi_1$ is more negative, than for models computed far from the resonance, and this effect seems to have great influence on the observed O1 phase lag distribution.

We confirm the finding of Ogloza *et al.* (2000) and Simon (1984), that the $\Delta\Phi_1$ is a good indicator of the pulsational mode that is independent of and supplemental to the usually used relative Fourier decomposition coefficients, R_{21}, Φ_{21}, etc). In principle, it is also a good criterion for identifying second overtone pulsators. However, no O2 Cepheids have been detected in the Galaxy, but there are a number of candidates in the Magellanic Clouds. For an independent confirmation of their status as O2 on the basis of the phase lag it would be necessary to acquire radial velocity data on these objects.

Ultra-low amplitude Cepheids would be easily discernible based on their phase lag. Our work predicts that ULA Cepheids pulsating in the fundamental mode and close to the fundamental red edge, would feature a greater phase difference, and would lie below the observed range [−0.2; −0.4] of the large-amplitude Cepheids. ULA first overtone Cepheids (at the blue edge) would be similarly separable, except in the

vicinity of the 'overtone' resonance. Therefore obtaining radial velocity data and existing light curve parameters could further prove their nature, *i.e.*, radial pulsation. Unfortunately, getting V_r curve for a small amplitude Cepheid in the MC remains a huge technological challenge.

Our survey has produced concurrently a rather complete theoretical overview of the nonlinear Cepheid instability strip, which delineates the regions of F, O1, O2 pulsation, of F&O1 and O1&O2 beat pulsation, and regimes of hysteresis, such as the 'either F or O1' regions and 'either O1 or O2' regions. These findings will be presented in a separate paper (Szabó & Buchler 2007, in preparation).

It is a pleasure to thank Peter Wood and Zoltán Kolláth for valuable discussions, as well as Pawel Moskalik for making the observed data available and his comments on the nature of IR Cep and V950 Sco. This work has been supported by NSF (AST03-07281 and OISE04-17772) at UF. RSz acknowledges the support of a Hungarian Eötvös Fellowship. We are grateful to the the Hungarian NIIF Supercomputing Facility and to the UF High-Performance Computing Center for providing computational resources and support without which we would not have made such extended survey of full amplitude models.

REFERENCES

Alexander, D. R., & Ferguson, J. W. 1994, ApJ, 437, 879
Antonello, E., & Aikawa, T. 1995, A&A, 302, 105
Antonello, E., & Kanbur, S. M. 1997, MNRAS, 286, L33
Antonello, E., & Morelli, P. L. 1996, A&A, 314, 541
Asplund, M., Grevesse, N., & Sauval, A.J. 2005, in *Cosmic Abundances as Records of Stellar Evolution and Nucleosynthesis*, ASP Conf. Ser. 336, 25
Beaulieu, J. P., Buchler, J. R., & Kolláth Z. 2001, A&A, 373, 164
Bono, G., Caputo, F., Cassisi, S., Marconi, M., Piersanti, L., & Tornambè, A. 2000, ApJ, 543, 955
Buchler, J. R. 1993, in *Nonlinear Phenomena in Stellar Variability*, Eds. M. Takeuti & J.R. Buchler (Kluwer: Dordrecht), repr. from ApSS 210, 1
Buchler, J. R. 1997, in "Astrophysical Returns From Microlensing Projects", Eds. R. Ferlet, J.P. Maillart & B. Raban, Editions Frontières, Gif-s-Yvette, p. 181
Buchler, J. R., & Kolláth, Z. 2002, ApJ, 573, 324
Buchler, J. R., & Kovács, G. 1986, ApJ, 308, 661
Buchler, J. R., & Szabó, R. 2007, ApJ, accepted
Buchler, J. R., Wood, P. R., Keller, S., & Soszyński, I. 2005, ApJ, 631, 151
Castor, J. I., 1968, ApJ, 154, 793
Fernie, J. D., Beattie, B., Evans, N. R., & Seager, S., 1995, IBVS, 4148 http://www.astro.utoronto.ca/DDO/research/cepheids
Feuchtinger, M., Buchler, J. R., & Kolláth, Z. 2000, ApJ, 544, 1056
Girardi, L., Bressan, A., Bertelli, G., & Chiosi, C. 2000, A&AS, 141, 371
Grevesse, N., & Anders, E. 1991, in *Solar Interior and Atmosphere*, Univ. of Arizona Press, p. 1227
Iglesias, C. A., & Rogers, F. J. 1996, ApJ, 464, 943, www-pat.llnl.gov/Research/OPAL/
Kolláth, Z., Beaulieu, J. P., Buchler, J. R., & Yecko, P. 1998, ApJ, 502, L55
Kolláth, Z., Buchler, J. R., Szabó, R., & Csubry, Z. 2002, A&A, 385, 932
Kovács, G. 2000, A&A, 360, L1
Moskalik P., & Buchler J. R. 1989, ApJ, 341, 997
Moskalik P., & Buchler J. R. 1990, ApJ, 355, 590
Moskalik P., & Buchler J. R. 1991, ApJ, 366, 300
Moskalik, P., & Ogloza, W. 2000, ASP Conf. Ser. 203, 237
Nardetto, N., Mourard, D., Kervella, P., Mathias, Ph., Mérand, A., & Bersier, D. 2006, A&A, 453, 309
Ngeow, C.-C., Kanbur, S. M., Nikolaev, S., Tanvir, N. R., & Hendry, M. A. 2003, ApJ, 586, 959
Ogloza, W., Moskalik, P., & Kanbur, S. 2000, ASP Conf. Ser. 203, 235
Simon, N. R. 1984, ApJ, 284, 278
Simon, N. R., & Davis, C. G. 1983, ApJ, 266, 787
Simon, N. R., & Moffett, T. J. 1985, PASP, 97, 1078
Soszynski, I., Udalski, A., Szymanski, M., Kubiak, M., Pietrzynski, G., Wozniak, P., & Zebrun, K. 2001, AcA, 50, 451
Stellingwerf, R. 1975, ApJ, 195, 441
Turner, D. G., Savoy, J., Derrah, J., Abdel-Sabour Abdel-Latif, M., & Berdnikov, L. N. 2005, PASP, 117, 207
Udalski, A., Soszynski, I., Szymanski, M., Kubiak, M., Pietrzynski, G., Wozniak, P., & Zebrun, K. 1999, AcA, 49, 1
Yecko, P. A., Kolláth, Z., & Buchler, J. R. 1998, A&A, 336, 553